

# Study on the Output Current for Electrochemical Low-energy Neutrino Detector with Regards to Oxygen Concentration

Shoya Suda<sup>1\*</sup>, Kenji Ishibashi<sup>1</sup>, Eka Sapta Riyana<sup>1</sup>, Yani Nur Aida<sup>2</sup>, Shohei Nakamura<sup>3</sup>, Yoichi Imahayashi<sup>4</sup>

<sup>1</sup>Department of Applied Quantum Physics and Nuclear Engineering, Kyushu University, Fukuoka, Japan; <sup>2</sup>SyarifHidatattullah State Islamic University, Jakarta, Indonesia; <sup>3</sup>Infrastructure System Company, Hitachi, Tokyo, Japan; <sup>4</sup>Mitsubishi Electric, Tokyo, Japan

## ABSTRACT

**Background:** Experiments with small electrochemical apparatus were previously carried out for detecting low-energy neutrinos under irradiation of reactor neutrinos and under natural neutrino environment. The experimental result indicated that the output current of reactor-neutrino irradiated detector was appreciably larger than that of natural environmental one. Usual interaction cross-sections of neutrinos are quite small, so that they do not explain the experimental result at all.

**Materials and Methods:** To understand the experimental data, we propose that some biological products may generate AV-type scalar field  $B^0$ , leading to a large interaction cross-section. The output current generation is ascribed to an electrochemical process that may be assisted by weak interaction phenomena. Dissolved oxygen concentrations in the detector solution were measured in this study, for the purpose of understanding the mechanism of the detector output current generation.

**Results and Discussion:** It was found that the time evolution of experimental output current was mostly reproduced in simulation calculation on the basis of the measured dissolved oxygen concentration.

**Conclusion:** We mostly explained the variation of experimental data by using the electrochemical half-cell analysis model based on the DO concentration that is consistent to the experiment.

**Keywords:** Neutrino, Weak interaction, Weak charge, Scalar field, Electrochemical reaction

## Introduction

Neutrinos are neutral particles which have extremely small interaction cross-sections, for instance, of the order of  $10^{-44} \text{ cm}^2 (E\text{-MeV}^{-1})$  [1]. In the quantum field theory, electromagnetic interaction potential  $A_\mu$  is generated by Vector (V) type interaction current as  $\bar{\psi}\gamma_\mu\psi$ , where  $\mu$  is one of space-time directions ( $t, x, y, z$ ),  $\psi$  is a wave function of particle and  $\gamma_\mu$  is a V-type gamma matrix. The V-type current propagates through a propagator with massless boson (photon) and generates the potential in the  $\mu$  direction. In contrast, interactions of neutrinos are explained by the standard model [2-4] by using Vector-Axial Vector (V-AV) type interaction to explain the spin direction (helicity), where quite massive gauge bosons are introduced into propagator through the spontaneous symmetry breaking. The interaction current is  $\bar{\psi}\gamma_\mu(1-\gamma_5)\psi = \bar{\psi}\gamma_\mu\psi - \bar{\psi}\gamma_\mu\gamma_5\psi$ , and

## Technical Paper

**Received** July 17, 2015  
**Revision** October 11, 2016  
**Accepted** October 24, 2016

**Corresponding author:** Shoya Suda

Department of Applied Quantum Physics and Nuclear Engineering, Kyushu University, 744, Motooka, Nishi-ku, Fukuoka 819-0395, Japan  
Tel: +81-92-802-3484,  
Fax: +81-92-802-3484,  
E-mail: ssuda@kune2a.nucl.kyushu-u.ac.jp

This is an Open-Access article distributed under the terms of the Creative Commons Attribution Non-Commercial License (<http://creativecommons.org/licenses/by-nc/4.0>) which permits unrestricted non-commercial use, distribution, and reproduction in any medium, provided the original work is properly cited.

Copyright © 2016 The Korean Association for Radiation Protection

the latter term with  $\gamma_5$  expresses AV-type current. The V-AV type current forms V-AV type potential. It is noted that the weak charge has completely the same value as the electric charge  $e$  in the electromagnetic interaction.

Our group previously carried out the experiments with small electrochemical apparatus containing biological materials for detecting low-energy neutrinos under irradiation of reactor neutrinos and under natural neutrino environment [5]. The experimental result indicated that the output current of reactor-neutrino irradiated one was appreciably larger than that of the other. Since the interaction cross-sections of neutrinos are quite small, so that the experimental result is inexplicable by the usual weak interaction. There may exist strange phenomena for very low-energy neutrinos under a certain condition.

To understand the experimental data, we proposed an electrochemical model with assistance of certain weak interaction. It comes from simple assumptions on the weak neutral field  $B^0$  and normal electrochemical current generation process. Oxygen behavior in the detector is considered to play an important role in the output current generation. However, we have measured the dissolved oxygen concentration at single location in the detector solution so far, and applied the result as spatially uniform distribution for the output current analysis [6]. In this study, we attempt to measure the dissolved oxygen concentration at different location, and make clear the current generation process with a half-cell analysis model [6].

### Assumptions on Weak Interaction

The previous experiment [5] of our group is explained briefly. The results are shown in Figure 1. This indicates that the output current in the upper part (reactor-neutrino irradiation) is clearly larger than that of the lower (natural neutrino environment). The difference suggests that low-energy neutrino effect appears under a special condition.

Qualitative assumptions were made for the weak interaction to explain the experimental data. (1) A neutrino is composed of two types of internal constituent particles of weak charge type  $\nu_c$  and weak dipole moment one  $\nu_a$ . Both  $\nu_c$  and  $\nu_a$  generate the neutral field  $B^0 \approx -\partial^\mu A_\mu$ , but the fields basically cancel out in the region outside the neutrino. (2) Each constituent particle has motions of V- and AV-types, which serve as time-like and spatial-like movements, respectively. Quantities such as S matrix (for example [7]) for interaction cross-

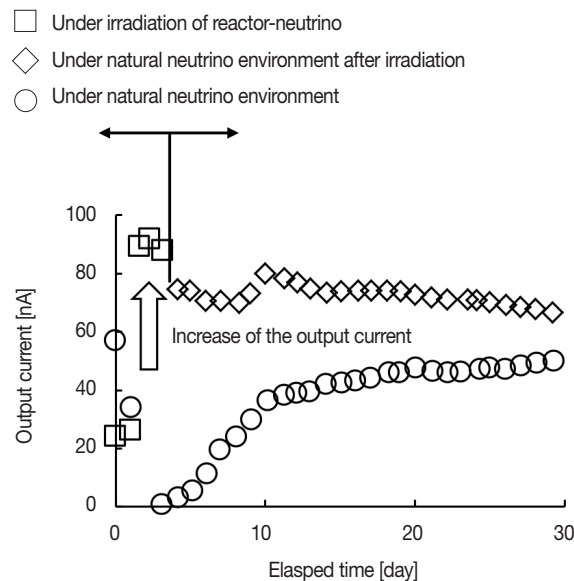


**Fig. 1.** Experimental data of low-energy neutrino detection. The output current in the upper part (reactor-neutrino irradiated one) is clearly larger than that in the lower.

sections may be defined by eigenvalue of V- and AV- matrices. The contribution to S matrix from V motion basically offsets that from AV, leading to the quite small interaction cross-section. This may be expressed by the function of massive bosons in the weak interaction.

The biological products such as raw silk may accumulate a large amount of charge-type neutrino fragments ( $\nu_c$ ) therein, and produce a considerable quantity of  $B^0$  in AV-type. The concentration of  $\nu_c$  has not been measured so far. However, the experimental data suggest us that raw silk should accumulate a sufficient amount of neutrino fragments through interaction with quite low energy environmental neutrinos. The strong  $B^0$  causes imbalance of S matrix, and make the interaction cross-section large. The resultant interaction cross-section may be comparable to the electromagnetic interactions at maximum, since the magnitude of charge values is the same for the weak and electromagnetic interactions. The experimental results possibly suggest that biological products like raw silk may generate AV-type scalar field  $B^0$ . The field is equivalent to Nakanishi-Lautrap field in the quantum theory of electromagnetic interaction [8].

### Electrochemical Reactions for Output Current

The detection mechanism is considered to be based on the electrochemical reaction which is assisted by the weak inter-

action. A gold electrode (anode) and a carbon electrode (cathode) are set at a distance of 1 cm in purified water of 50 g in the detector. Biological product of raw silk in total amount of 1 g is placed around the anode. A picture of the detector and dissolved oxygen (DO) meter is shown in Figure 2. Sche-



Fig. 2. Picture of the detector appearance and DO meter in incubator.

matic view of the detector is shown in Figure 3. A DO probe can be installed in either gold or carbon side at the time of oxygen concentration measurement. The incubator keeps the temperature constant at 27°C.

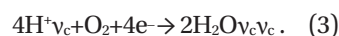
A neutrino of which cross-section is augmented under  $B^0$  may dissociate a water molecule as



The negative ions  $OH^- \nu_d$  may produce a reaction making use of energy difference of  $B^0$  between regions inside and outside the gold plate as



If  $B^0$  and  $\nu_d$  do not take part in the reaction, the reduction reaction cannot occur because of its original endothermic nature. The positive ions  $H^+ \nu_c$  make the exothermal reaction around the cathode as



The output current may be generated by the sequence of Equations 1-3. When Equation 2 makes progress with cata-

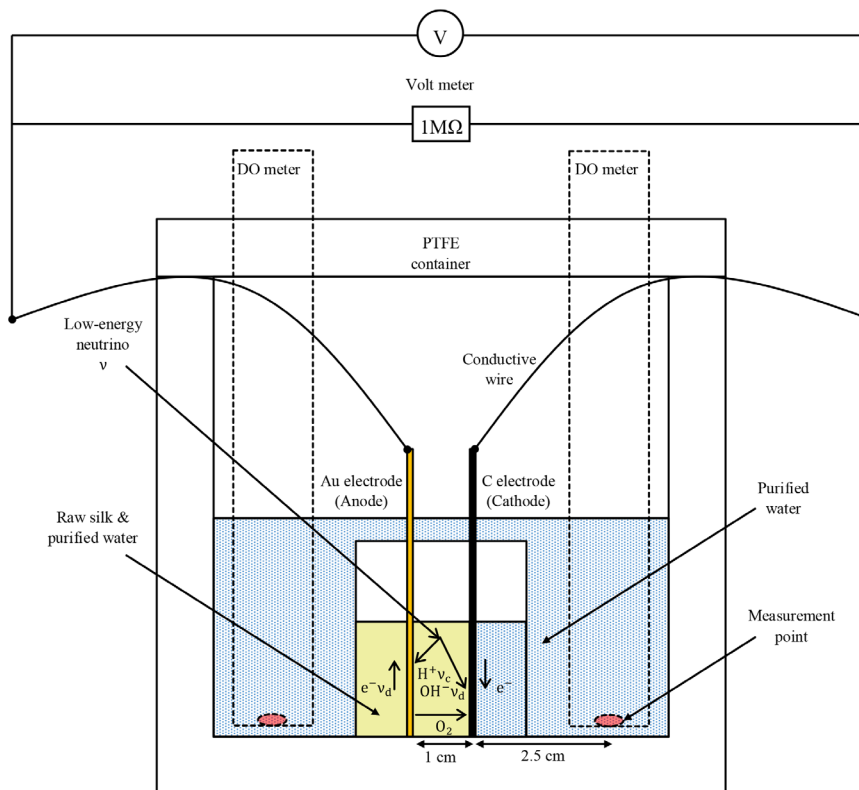


Fig. 3. Illustration of the low-energy neutrino detector. Raw silk arranged around an anode generates  $B^0$  field. When low-energy neutrino enters into this region, it is supposed to be dissociated into two constituent particles.

lytic-like effect of  $B^0$  and  $v_d$ , the reaction Equation 3 may work according to Butler-Volmer equation [8] in electrochemistry, being dependent on the temperature. Under the half-cell analysis model, the output current takes the form of

$$I(t) \approx P [C_{H+vc}(t)]^{n_H} [C_{O_2}(t)]^{n_O} \exp \left( - \frac{\Delta G + 4\alpha E(t)}{k_B T} \right) \quad (4)$$

where  $C_{H+vc}$  and  $C_{O_2}$  are concentrations (mol/cc) of the reactants,  $n_H$  and  $n_O$  are reaction orders,  $E$  is an electrode potential,  $P$  is a velocity constant,  $\alpha$  is a shift factor, and  $\Delta G$  is an activation energy of Equation 3. The value  $\Delta G$  is determined from experiments at different temperatures, by slope of the Arrhenius plot where the logarithmic current  $\log I$  is plotted as a function of  $1/T$ .

## Measurement of Dissolved Oxygen Concentration

To know information on  $C_{O_2}$ , we measured dissolved oxygen (DO) concentration with a DO meter based on a diaphragm type galvanic cell method. The measurement location is shown in Figure 3. The DO meter was set in purified water region in either the anode and the cathode side for the purpose of making clear the concentration difference. The experimental data are shown in Figure 4. The DO concentration is expressed by relative value (%) against equilibrium DO concentration under atmospheric pressure air. The DO concentration near the anode was comparable to the previous experiment [9].

The DO concentration in the anode side increases to a val-

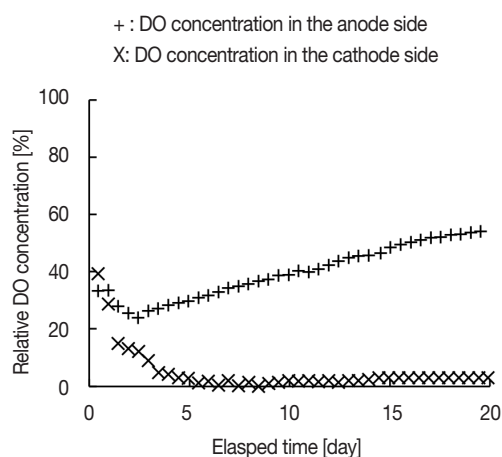


**Fig. 4.** Experimental data of DO concentration measurement. DO concentration in the anode side is increasing, whereas that in the cathode one decreasing.

ue about 50%, whereas that in the cathode decreases to 1-3%. The former behavior is considered to reflect the production of oxygen in Equation 2. The latter one may correspond to consumption thereof. The production and consumption of oxygen lead to difference in the concentration. The DO concentration difference shows therefore time dependence according to the amount of conducted electrons. Oxygen diffusion is expected to take place from the anode to the cathode corresponding to the electron flow in the closed circuit outside the container in Figure 2.

## Electrochemical Simulation

For analyzing the detector output, we took the measured concentrations of oxygen molecules into account, and simulated the detector output using quantities of  $P, \alpha, n_H, n_O$  in Equation 4 as adjustable parameters. The values are summarized in Table 1. These results are shown in Figure 5 by a

**Table 1.** The Values of the Parameters used for Both of the Simulation of Irradiated One and the Other

| Parameters                      | Values                                    |
|---------------------------------|---|
| $P$ : Velocity constant         | $1.6 \times 10^{-36} [A \cdot cc^{-2.5}]$ |
| $\alpha$ : Shift factor         | 1   |
| $n_H$ : Reaction order of H     | 1.5                                       |
| $n_O$ : Reaction order of $O_2$ | 1   |

- Under irradiation of reactor-neutrino
- ◇ Under natural neutrino environment after irradiation
- Under natural neutrino environment

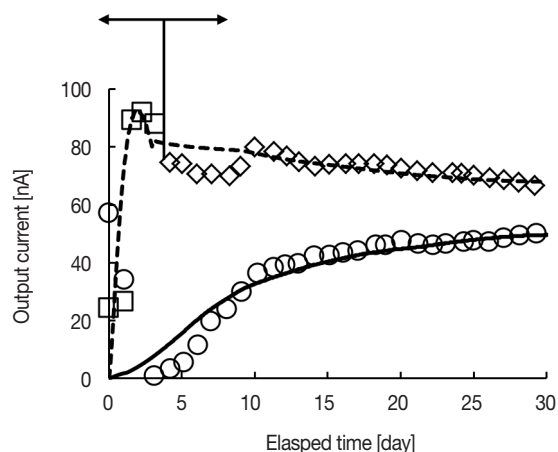


**Fig. 5.** The experimental data and the calculated results from electrochemical analysis. The calculated results are shown as solid line or dashed line reproduce the experimental data are represented by square.

solid line for the data under natural neutrino environment. The time evolution of experimental data was mostly reproduced in the simulation. The dashed line in the same figure was calculated by assuming a certain low-energy neutrino flux under irradiation of reactor neutrinos for three days. In this estimation, we set the flux of low-energy neutrinos under irradiation as thirty times as high as that in the environment. In addition, we set DO concentration of irradiated one by one third in the environment current for fitting. The higher output current may bring about the more consumption rate of oxygen. The output current decreases from the third to tenth day. This might be caused by the effect of vibrating motion of the detector during transportation from the experimental site to our laboratory. The convergence of the output current may be caused to reach an electrochemical equilibrium state.

## Conclusion

Experiments were carried out to measure dissolved oxygen (DO) concentration at location in the anode and cathode sides of the detector. It was confirmed that DO concentration increases in the anode side while decreasing in the cathode one. This imbalance indicates diffusion of oxygen molecule from the anode to the cathode corresponding to electric current flow through conductive wires. We mostly explained the variation of experimental data by using the electrochemical half-cell analysis model based on the DO concentration that is consistent to the experiment.

## Acknowledgements

The authors express our gratitude to the staff of the laboratory of radiation physics and measurement for cooperating of the experiment.

## References

1. Formaggio JA, Zeller GP. From eV to EeV: Neutrino cross-sections across energy scales. *Rev. Mod. Phys.* 2013;84:1307-1314.
2. S. L. Glashow. Partial-symmetries of weak interactions. *Nucl. Phys.* 1961;22:579-588.
3. Weinberg S. A model of Lepton. *Phys. Rev. Lett.* 1967; 19:1264-1266.
4. Salam A. Weak and Electromagnetic Interactions. 8th Nobel Symposium. Lerum, Sweden. May 19-25, 1968.
5. Liu W, Ishibashi K, Arima H, Iijima T, Katano Y, Naoi Y. Possible detection of natural neutrinos by use of small apparatus. *J. Nucl. Sci. Technol.* 2004;41:487-490.
6. Aida N, et al. Proposed analysis on output currents of electrochemical apparatus with regards to weak interaction. *Memoirs of the Faculty of Engineering Kyushu University.* 2013; 73:27-37.
7. Weinberg S. *The Quantum theory of fields.* 6th Ed. Cambridge, UK. Cambridge University Press. 1996;107-291.
8. Nakanishi N. Covariant quantization of the electromagnetic field in the Landau gauge. *Prog. Theor. Phys.* 1966;35:1111-1116.
9. Bard AJ, Faulker LR. *Electrochemical methods fundamentals and applications.* 2nd Ed. New York, NY. John Wiley & Sons. 2001: 92-107.
10. Liu W. Study on detection of environmental neutrinos by means of miniaturized apparatus based on electrochemical reaction. *Kyushu University. Doctoral Thesis.* 2004;54-94.